Published in AJSE, Vol: 24, Issue:2
Received on 30th June 2024
Revised on 25th May 2025
Published on 31th May 2026

AIUB JOURNAL OF SCIENCE AND ENGINEERING
ISSN: 1608 - 3679 (print) 2520 - 4890 (Online)
https://doi.org/10.53799/q83e4415

The growth of α-Fe(Si) nanocrystalline grains as a function of temperature in amorphous $Fe_{76.5-x}Nb_xCu_1Si_{13.5}B_9$ (x=1, 3, 5, 7) alloys and study their hardness

M. M. Rana, Md. Sarowar Hossain, Md. Ehasanul Haque, M. R. Hassan, M. H. Rizvi, M. N. I. Khan, A. Z. Ziauddin Ahmed and M. A. Hakim

Abstract- An amorphous ribbon of composition $Fe_{76.5-x}Nb_xCu_1Si_{13.5}B_9$ (x = 1, 3, 5, and 7) was synthesized by the rapid solidification of chilling metallic liquids by melt spinning technique. The crystallization onset temperatures for the studied samples have been evaluated from Differential Scanning Calorimetry (DSC). X-ray diffraction pattern confirms the growth of the nano-crystalline Fe(Si) phase on the amorphous matrix. Moreover, the microstructure and grain size for all samples have been determined by field emission scanning electron microscopy (FESEM). It is observed that the crystallization phase and grain sizes increase due to heat treatment. However, the sizes of grains are reduced for the replacement of Fe^{3+} with a high amount of Nb^{5+}. In addition, the hardness also increases along with the increase of Nb content and heat treatment. Finally, a brief study on crystalline phase kinetics and its controlling parameters for the Finemet® alloy system has been explored.

Index Terms- Microstructure, Annealing, Amorphous ribbon, Crystallization, Microhardness.

M. M. Rana
Dept. of Theoretical Physics, University of Dhaka, Dhaka, Bangladesh
masud5972@gmail.com

Md. Sarowar Hossain
Department of Natural Science (Physics), American International University-Bangladesh, Dhaka, Bangladesh
sakil_phy@aiub.edu

Md. Ehasanul Haque
Department of Industrial and Production Engineering, American International University-Bangladesh, Dhaka, Bangladesh
ehasanul@aiub.edu

M. R. Hassan
Rooppur Nuclear Power Plant, Pabna, Bangladesh
Department of Physics, Khulna University of Engineering and Technology, Khulna, Bangladesh
rabifagun@gmail.com

M. H. Rizvi
North Carolina State University, USA
Dept. of NCE, Bangladesh University of Engineering & Technology, Dhaka, Bangladesh
rizvimme0711017@gmail.com

M. N. I. Khan
Material Science Division, Atomic Energy Centre, Bangladesh
ni_khan77@yahoo.com

A. Z. Ziauddin Ahmed
Department of Basic Sciences, Primeasia University, Dhaka, Bangladesh
azzahmed@primeasia.edu.bd

M. A. Hakim
Dept. of NCE, Bangladesh University of Engineering & Technology, Dhaka-1000, Bangladesh
hakim.akm@gmail.com

I. INTRODUCTION

Finemet® is known as a Fe-based alloy with fine nanocrystalline grains which was first invented by Yoshizawa et al. in 1988 [1]. This system has tremendous applications in the electrical industry. In general, this system is a class of metallic glass materials that do not have long-range atomic order and structurally they are amorphously characterized like that of liquid state. These materials are a great option for high-frequency electronic applications due to their ultrasoft magnetic properties [2-4]. However, the microstructure of this system controls the magnetic properties of this system following the Random Anisotropy model proposed by Herzer et al [5]. In addition, this alloy system exhibits high initial permeability, high saturation magnetization, low core loss, and low coercivity, simultaneously [6, 7]. Due to high permeability, they are used to make energy-saving materials like Electromagnetic interference **(**EMI) filters, magnetic shielding sheets, common mode chokes, current sensors, electromagnetic wave absorbents, and magnetic sensors. The low core loss property of these alloys enables them for high-performance device applications like magnetic amplifiers, surge protectors, high-voltage pulse transformers, and pulse power cores. The low magnetostriction is useful for high-frequency tools like high-frequency power transformers, active filters, smoothing choke coils, and accelerator cavities. Ribbon-shaped Finemet® samples are typically created by rapidly chilling liquid metallic alloys with a very high rate of chilling (10^5–10^6 K/s). Therefore, nucleation and growth of the crystalline phase are kinetically bypassed in the as-cast sample and no microstructural inhomogeneities are observed. However, the amorphous state is metastable, and researchers have been paying attention to 5-10% Si and 75-78% Fe to formulate Fe(Si) based alloys. In addition, some nanocrystalline grains can be dispersed easily in a residual amorphous matrix with increasing temperature in these Fe-Si-B based alloys, and α-Fe(Si) and Fe(B) phases are considered as primary and secondary crystallization respectively [8-10]. Subsequent annealing above the recrystallization temperature develops a Fe-Si solid solution of BCC structure embedded in the amorphous matrix of parent Fe-Si-B-based alloys and grains of approximately 10-15 nm are observed. Differential scanning calorimetry is the most common technique to determine the phase transition temperatures of crystallization [11]. The crystallization follows the route as Amorphous → Cu rich area → the nucleation of bcc Fe from Cu bcc → Fe(-Si). The reaction kinetics can be controlled by adding Cu and Nb in the parent Fe-Si-B-based alloy. Here, Cu promotes nucleation by developing the BCC Fe-Si phase while Nb acts as the grain

growth inhibitor. Finally, a nanocrystalline ultrafine soft grain of about 10-25 nm [9] could be achieved. In addition, the compositional variation leads to significant changes in both the temperatures of α-Fe crystals precipitation and the Curie temperature, T_C. It is well known that the excellent soft magnetic properties of Finemet-type alloys are microstructure-dependent [12,13], which could be controlled by the synthesis procedure and thermal treatment. Several researchers observed the magnetic properties of these alloys under different annealing conditions [14-16]. In addition, certain correlations between thermal and magnetic properties are observed in amorphous and nanocrystalline Finemet® microwires [17,18]. Therefore, analyzing the evolution of fundamental characteristics of Finemet® materials (phase composition, microstructures, distribution of elements within phases, etc.) is of great importance to achieve the expected magnetic properties.

In this paper, we evaluate the structure and microstructures of a Finemet® composition due to the substitution of a small amount of Nb at Fe along with the growth of α-Fe(Si) nanocrystalline grains in the amorphous due to heat treatment. The nucleation of crystallization and temperatures of structural transformation are studied by differential scanning calorimetry (DSC). In addition, the hardness of the synthesized samples due to Nb doping was observed.

II. EXPERIMENTAL:

Metglass ribbon samples of nominal composition $Fe_{76.5-x}Nb_xCu_1Si_{13.5}B_9$ (x= 1, 3, 5, 7) were synthesized. The starting materials of analytical grade Fe, Nb, Cu, Si, and B were collected from Johnson Mathey (Alfa Aesar) with purity of 99.98%, 99.5%, 99%, 99.9%, and 99.5% respectively.

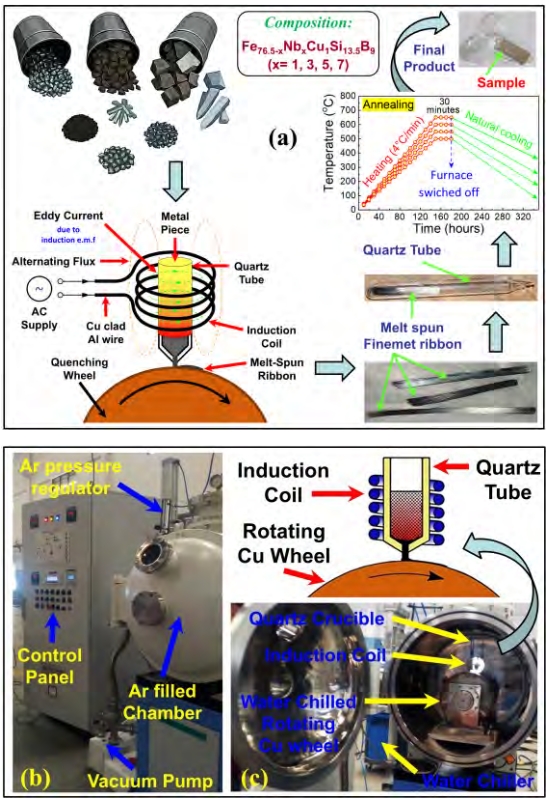

Fig. 1. Sample preparation as depicted by **(a)** Flow chart of synthesization, and components of apparatus showing **(b)** pressure-controlled chamber filled by Ar gas and **(c)** copper wheel attached with an induction coil and vacuum sealed quartz tube with raw materials.

The stoichiometric amounts of these raw materials were weighed very carefully for the stated composition and kept inside a quartz tube under an argon pressure of 0.5 atm. Afterwards, the raw materials were melted at 1450 °C by an induction furnace as shown in Fig. 1. The liquid cast was rapidly solidified by ejecting on a spinning Cu wheel that was under 35 turns/second speed. Finally, the ribbon-shaped samples with dimensions of 6 mm width and 20 to 22 µm thickness were prepared by melt spinning technique for the present study. The as-cast products of the samples were then sealed in evacuated quartz tubes and annealed at 500℃, 550℃, 600℃, and 650℃ temperatures respectively. The differential scanning calorimetry (DSC) measurement for the present ribbon samples was performed in the standard instrument of model DSC-2960 SDT, (USA), and the crystallization temperatures were confirmed from the DSC data. Additionally, the structure was analyzed by recording X-ray spectra for the samples using the Philips X'Pert Pro (PW3040) diffractometer with Cu-Kα radiation (λ=1.5405 Å) over a scanning range of $30° \leq 2\theta \leq 90°$. Moreover, the microstructures of the synthesized samples were studied using a Field Emission Electron Microscope (FESEM) of model JEOL JSM 7600F with an energy ranging from 0.2 keV to 40 keV and operational accelerating voltage of 200V to 30kV. Hardness tests were finally performed on samples synthesized and annealed at 650℃ using the nano-indentation technique with a Digital Micro Vickers Hardness Tester (Vexus MHV-1000Z Series). The hardness values were calculated based on the stiffness obtained from the unloading curve at a final indentation depth of 1000 nm. Additionally, the experiment was conducted at three different locations on each sample, with 10 indents at each position, to ensure the accuracy and reliability of the hardness measurements.

III. RESULT AND DISCUSSIONS

A. Differential Scanning Calorimetry (DSC)

Differential scanning calorimetry (DSC) with a constant heating rate of 20ºC/min has been performed on the selected composition of $Fe_{76.5-x}Nb_xCu_1Si_{13.5}B_9$ for x = 3, 5, and 7, and the temperature ranging from 100℃ to 800℃. Fig. 2 illustrates the DSC curve for the studied samples and the observed exothermic peaks correspond to the crystallization. Each of the three samples shows two subsequent peaks, signifying the occurrence of primary and secondary crystallization at different temperatures. In general, the exothermic peak (P_1) at a lower temperature as depicted in Fig.2(a) indicates the formation of the α-Fe(Si) phase, a body-centered cubic (BCC) mixture of silicon and iron. Moreover, the higher temperature exothermic peak, labeled P_2 in Fig. 2(a), corresponds to the formation of the Fe-B crystalline phase in the Finemet samples. During annealing, Finemet partially crystallizes, transforming some of its amorphous structure into the crystalline α-Fe(Si) phase, which is typically dispersed within the remaining amorphous matrix. However, as the Nb content increases, the primary and secondary crystallization temperatures move to a higher temperature range, suggesting that adding Nb improves the alloy's thermal stability. As a result, the primary crystallization temperature moves to 589°C for the sample with a higher Nb content (x = 7), making the crystallization event more challenging than it was for the sample with a

lower Nb content of x = 5. The DSC thermogram in Fig. 2 shows that the secondary peak shifts to a higher temperature due to an increase in Nb content.

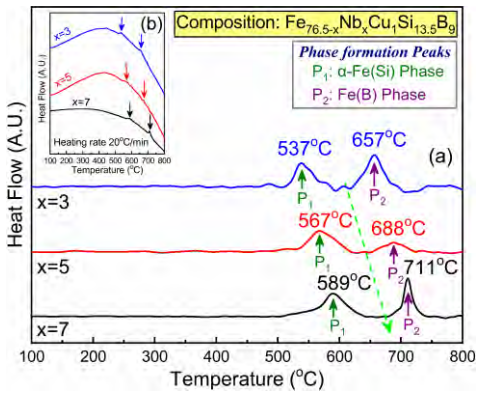

Fig. 2. DSC thermogram obtained for $Fe_{76.5-x}Nb_xCu_1Si_{13.5}B_9$ alloys with x=3, 5, and 7 that is illustrated by **(a)** phase formation temperatures and **(b)** at heating rate 20°C/min.

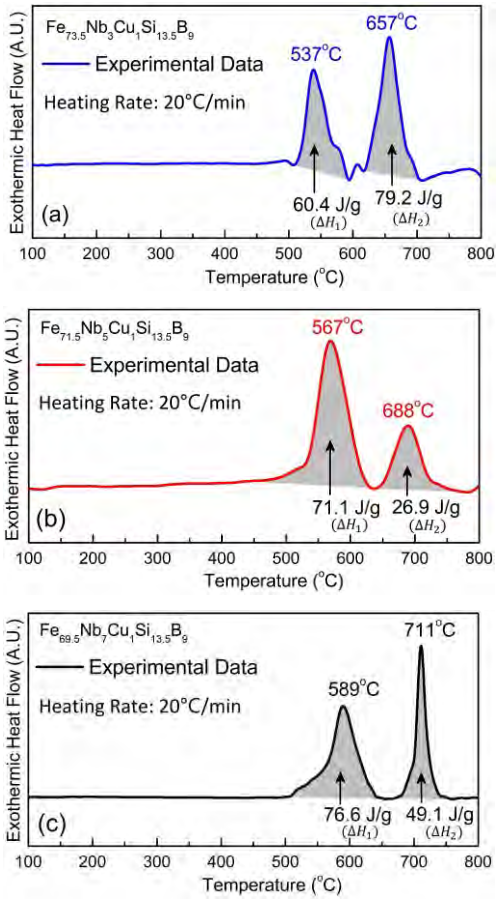

Fig. 3. Change of enthalpies evaluated from the area under the curve of exothermic peak originated during α-Fe(Si) crystallization in amorphous $Fe_{76.5-x}Nb_xCu_1Si_{13}$ alloys where **(a)** for x=3 **(b)** for x=5, and **(c)** for x=7.

The results of these crystallization temperatures have been presented in Table I. Moreover, the reaction kinetics have been studied from the area under the curve of the reaction peaks as shown in Fig. 3 for the studied samples which evaluate the enthalpy (ΔH_1) during the α-Fe(Si) phase formation in these amorphous samples. It is observed from Fig.3(a) that the value of ΔH_1 is small ($\Delta H_1 = 60.4\,J/g$) for a high amount of Fe concentration (73.5 at.%) in $Fe_{73.5}Nb_3Cu_1Si_{13.5}B_9$ sample that is correlated to the early participation of α-Fe(Si). The enthalpy of phase formation, ΔH increases to $76.6\,J/g$ as Nb content goes up as in the sample $Fe_{69.5}Nb_7Cu_1Si_{13.5}B_9$. On the other hand, the value of ΔH_2 is higher (79.2 J/g) for the Fe-B crystalline phase formation in the composition $Fe_{73.5}Nb_3Cu_1Si_{13.5}B_9$. However, the addition of Nb in the parent composition increases the stability of the amorphous Fe-B phase, making it energetically more favorable (i.e., lowering the enthalpy). In general, Nb can react with B to form stable Nb-B compounds (such as Nb_3B_4), which removes B from the Fe-B phase [19]. This formation of stable Nb-B compounds effectively reduces the energy associated with the Fe-B interactions resulting in the reduction of enthalpy of the remaining Fe-B phase. Therefore, ΔH_2 for the composition $Fe_{71.5}Nb_5Cu_1Si_{13.5}B_9$ decreases to 26.9 J/g. Nevertheless, adding more Nb shows an unexpected result for the composition $Fe_{69.5}Nb_7Cu_1Si_{13.5}B_9$ in which ΔH_2 is slightly higher (49.1 J/g) than it is for the sample x=5. This result is attributed to the existing distortions, and metastable phases due to the larger atomic size of Nb compared to Fe. These factors contribute to higher internal energy within the Fe-B phase, manifesting as an increase in enthalpy.

TABLE I

Differential scanning calorimetric measured data for $Fe_{76.5-x}Nb_xCu_1Si_{13.5}B_9$ (x = 3, 5 and 7) showing crystallization temperatures for Primary phase (T_{p1}) and secondary phase (T_{p2}) and ΔH_1 is the enthalpy during primary phase (α-Fe(Si)) formation while ΔH_2 illustrate the enthalpy during the secondary phase formation.

Nb Content (x)	T_{p1} (°C)	T_{p2} (°C)	ΔH_1 (J/g)	ΔH_2 (J/g)	Heating rate (°C/min)
3	536	658	60.4	79.2	20
5	555	671	71.1	26.9	20
7	586	710	76.6	49.1	20

It appears that the fraction of α-Fe(Si) participation is strongly promoted by the increased Nb concentration from 3 to 7 at. %. It is widely acknowledged that in Fe-Si-B-based amorphous alloys, a significant quantity of α-Fe(Si) can be formed early in the crystallization process with the aid of Cu, and the remaining phases will form in a eutectoid process alongside the Fe-B phase [19]. Furthermore, a considerable quantity of B is trapped close to Nb atoms creating Nb-B bond [19] and losing its ability to aid in the formation of the Fe-B phase. Fig. 3 (b and c) confirms that an increase in Nb content increases the capacity of α-Fe(Si) formation during the first step in $Fe_{71.5}Nb_5Cu_1Si_{13.5}B_9$ and $Fe_{69.5}Nb_7Cu_1Si_{13.5}B_9$. Consequently, the investigated samples were annealed at 500°C, 550°C, 600°C, and 650°C, respectively. In all samples, the expected outcome is the growth of the α-Fe(Si) crystalline phase, where the Nb-B bond may help more than diffusion barriers.

B. Structure and microstructure analysis

The XRD patterns of $Fe_{76.5-x}Nb_xCu_1Si_{13.5}B_9$ (x = 1, 3, 5, and 7) alloys in as cast and annealed at 500°C, 550°C, 600°C and 650°C for 30 minutes are shown in Fig. 4 and 5 respectively. The peak broadening in the diffraction patterns obtained for the as-quenched samples (Fig. 4) indicates the existing amorphous phase. On the other hand, when amorphous material crystallizes, larger grains are formed and the broader peaks become narrower and sharper [20].

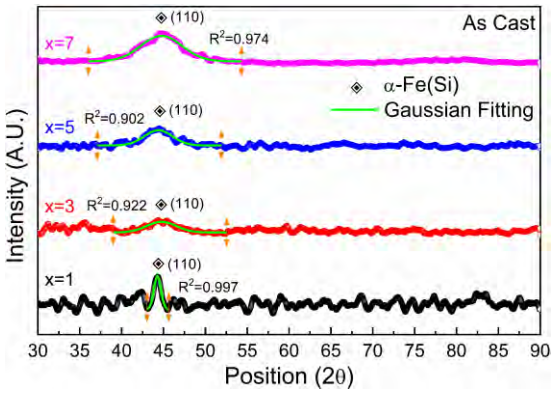

Fig. 4. XRD patterns of as-cast ribbon of $Fe_{76.5-x}Nb_xCu_1Si_{13.5}B_9$ where, x=1, 3, 5 and 7.

Therefore, the samples after the heat treatment exhibit crystalline peaks at $2\theta \approx 45°$ corresponding to the α-Fe(Si) phase as displayed in Fig. 5. In addition, this is identified as the characteristic diffraction peak of the (110) plane, which confirms the presence of a body-centered cubic (BCC) structure [21]. However, the diffraction patterns in Fig. 5 (a) illustrate the amorphousness of the composition with x=5 and 7 due to annealing at the lower temperature (T_a=500°C) while the other two samples (x=1 and 3) are partially crystallized during heat treatment at this temperature. In the progression of the annealing temperature, Fig. 5(b) represents the structures of all studied samples for T_a=550°C. Similar results are obtained at this temperature for the samples of x=5 and 7 except the sharpness and intensities of the (110) peak are increased for the samples of x=1 and 3. Therefore, a good coincidence with the DSC thermogram is observed as the crystallization temperature (T_{P_1}) for x=5 and 7 are 555°C and 586°C respectively and α-Fe(Si) phase formation is in hurdle again at T_a = 550°C for the samples for $x > 3$. However, an enhancement of this phase formation is observed in Fig. 5(c) followed by Fig. 5(d) when the annealing temperature is raised to higher values of 600°C and 650°C, respectively. Therefore, a complete crystallization of all samples has been achieved for T_a = 650°C as depicted in Fig. 2 (d).

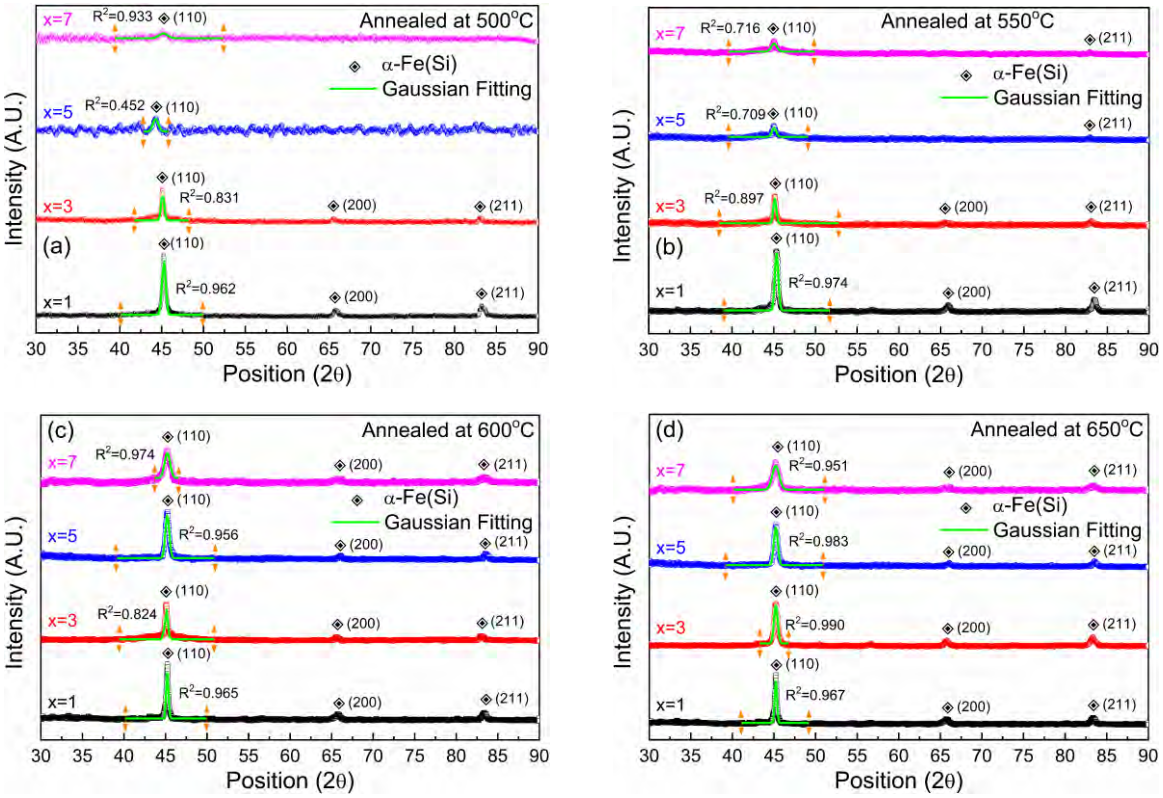

Fig. 5. XRD patterns of $Fe_{76.5-x}Nb_xCu_1Si_{13.5}B_9$ ribbon where, x=1, 3, 5, 7 annealed at **(a)** 500°C, **(b)** 550°C, **(c)** 600°C and **(d)** 650°C

In addition, the crystalline quality is further compared based on the crystallite size (D_{110}) and lattice strain (ε_L) along with dislocation density (δ_{110}) where $\delta_{110} = 1/(D_{110})^2$ for the studied samples. Here the values of D_{110} have been calculated for the XRD peak at (110) that corresponds to this α-Fe(Si) phase only and the Scherrer equation [22, 23] has been used as given,

$$D_{110} = \frac{k\lambda}{\beta cos\theta} \quad (1)$$

where θ is the Bragg angle of the (110) diffraction peak, k is the dimensionless constant, which typically has a value of 0.9, and λ is the wavelength of $Cu - k\alpha$ radiation, which has a value of 1.5418Å. β was determined through Gaussian fitting of the peaks at (110) in the data as shown in Fig.5. Furthermore, the lattice constant (C) can be determined using the formula $C = \lambda/(sin(\theta))$. Consequently, the lattice strain (ε_L) has been calculated by the relation.

$$\varepsilon_L = \frac{C - C_0}{C_0} \times 100 \quad (2)$$

where the value of C is constant for individual samples and C_0 is the lattice constant for an ideal strain-free sample. The obtained values of D_{110}, ε_L and δ_{110} are included in Table II. Here, it is observed that the values D_{110} are increased with the annealing temperature except for the sample x=3 in which D_{110} initially increases at $T_a = 500$°C and above which it

decreases. These variations of the α-Fe(Si) crystallites are depicted in Fig. 6(a) and the value of D_{110} is found to be in the ranges from 9.1 nm to 1.5 nm for the studied samples in the as-cast condition.

TABLE II

Structure and microstructural factors estimated from XRD data and SEM image recorded for $Fe_{76.5-x}Nb_xCu_1Si_{13.5}B_9$ (x=1, 3, 5 and 7) representing crystallite size (D_{110}), lattice strain (ε_L), dislocation density (δ_{110}) and grain sizes (D_{SEM}) as a function of heat treatment.

T_a (°C)	Nb Content (x)	D_{110} (nm)	ε_L	$\delta_{110} \times 10^{-4}$ $(nm)^{-2}$	D_{SEM} (nm)
As cast	1	9.1	0.01054	0.012	Amorphous
	3	2.1	0.04464	0.227	Amorphous
	5	2.2	0.04225	0.207	Amorphous
	7	1.5	0.06170	0.444	Amorphous
500	1	17.8	0.00528	0.003	118.4 ± 0.4
	3	21.3	0.00444	0.002	91.5 ± 2.6
	5	11.5	0.00835	0.008	Amorphous
	7	7.2	0.01302	0.019	Amorphous
550	1	18.4	0.00510	0.003	124.9 ± 1.7
	3	21.6	0.00437	0.002	106.8 ± 4.0
	5	14.5	0.00652	0.005	Amorphous
	7	12.9	0.00730	0.006	Amorphous
600	1	26.4	0.00358	0.001	--
	3	21.5	0.00437	0.002	--
	5	16.4	0.00574	0.004	63.8 ± 0.5
	7	11.5	0.00821	0.008	41.0 ± 0.7
650	1	26.5	0.00356	0.001	--
	3	15.9	0.00593	0.004	--
	5	23.1	0.00406	0.002	92.8 ± 2.3
	7	24.6	0.00381	0.002	49.1±0.2

The crystalline phase starts to grow inside these samples at $T_a \geq 500$℃. The volume fraction (%) of the crystallinity (V_{Cry}) has been calculated from the XRD spectra using the equation [24, 25] as given,

$$V_{cry} = \frac{I_{cry}}{I_{cry} + I_{am}} \quad (3)$$

where, I_{cry} and I_{am} are the integral intensities of diffraction peaks of the crystalline phase and amorphous phase, respectively.

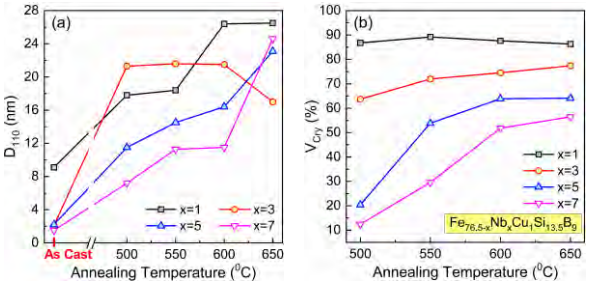

Fig. 6. Effect of annealing on the structures illustrated by the **(a)** variation of crystallite sizes (D_{110}) and **(b)** volume fraction (V_{cry}) evaluated for $Fe_{76.5-x}Nb_xCu_1Si_{13.5}B_9$ alloys where, x = 1, 3, 5, and 7.

The integral intensities of I_{am} have been obtained from the area under the curve of the XRD spectra for the as-cast samples as illustrated in Fig. 4. A Similar procedure over the crystalline spectra of Fig. 5 provides the values of I_{cry}. Therefore, Fig. 6(b) represents the values of V_{Cry} for the studied samples due to heat treatment at 500℃, 550℃, 600℃ and 650℃ respectively except for the sample x=1 in which V_{Cry} is degraded with T_a. The probable reason is that the growth of nanocrystals inside the sample for x=1 reaches a saturation level at 500℃ and the disordered phase starts to grow for the further increase of T_a. The annealing temperature promotes the growth of nanocrystals within the amorphous matrix of the microstructures. The average grain sizes and surface morphology of the composition $Fe_{76.5-x}Nb_xCu_1Si_{13.5}B_9$ with x = 1, 3, 5, and 7 are observed by the Field Emission Scanning Electron Microscopy (FESEM). The observed grains are nearly spherical and identical in all samples. Therefore, the appropriate sizes of the grains were determined by the line interpolation and calibration methods using ImageJ 1.50i software. Several particle sizes were estimated for this method, and the Gaussian equation was used to fit the size distributions as shown inset of Fig. 7. However, the as-cast sample in Fig. 7(a) does not show any sign of grain formation, and similar types of microstructures are observed in other studied samples in their as-cast form. Consequently, the as-cast sample for x = 1 was followed by the heat treatment of T_a=500ºC and 550ºC respectively and grains are observed. The growth of grains in these samples is visible depending on the annealing at different temperatures (T_{p1}) of phase formation as discussed above. Table II includes the values of average grain size for all the samples under study and it is observed that the grain size varied from 41.0 nm to 124.9 nm underlying causes of which are Nb doping and heat treatment. This result is concomitant with the increase in crystallite size evaluated from the XRD data. It is observed that the sample, x =1 for T_a = 500°C displays nano-grains of 118.4 nm as depicted in Fig. 7(b). Therefore, the annealing temperature, T_a is adequate to form α-Fe-Si nanograins with a body-centered cubic (BCC) structure in the sample, although the grains remain poorly defined due to agglomeration at this temperature. In this case, grain growth is inhibited, but the grains are highly agglomerated to minimize surface energy. However, the grains become more mature for T_a = 550°C, and the sizes of grains are increased to 124.9 nm in the same sample (Fig. 7(c)).

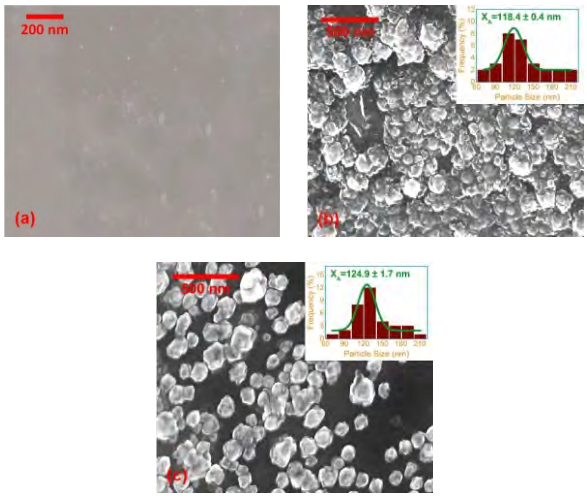

Fig. 7. Microstructures of $Fe_{75.5}Nb_1Cu_1Si_{13.5}B_9$ ribbon showing **(a)** as-cast surface along with annealed at **(b)** 500ºC and **(c)** 550ºC temperatures.

This result validates the kinetics of grain growth caused by heat treatment, and Fig. 8–10 shows a similar trend for the other compositions. Moreover, the increase in grain size with rising T_a is attributed to the diffusion of silicon into the

nanograins. Therefore, α-Fe(Si) nanograins are formed under various heat treatment conditions [26].

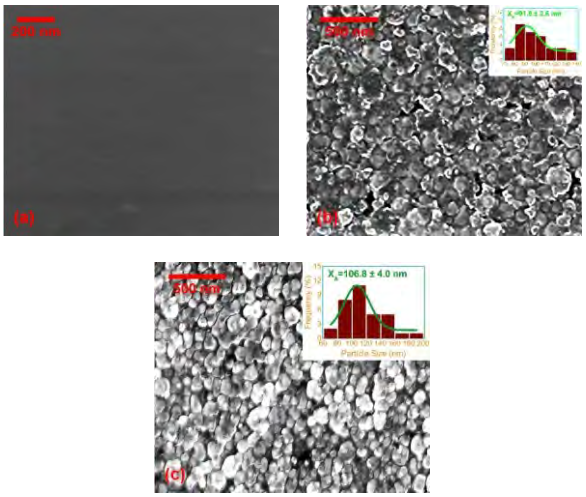

Fig. 8. Microstructures of $Fe_{73.5}Nb_3Cu_1Si_{13.5}B_9$ annealed at **(a)** 500ºC and **(b)** 550ºC and **(c)** 600ºC temperatures.

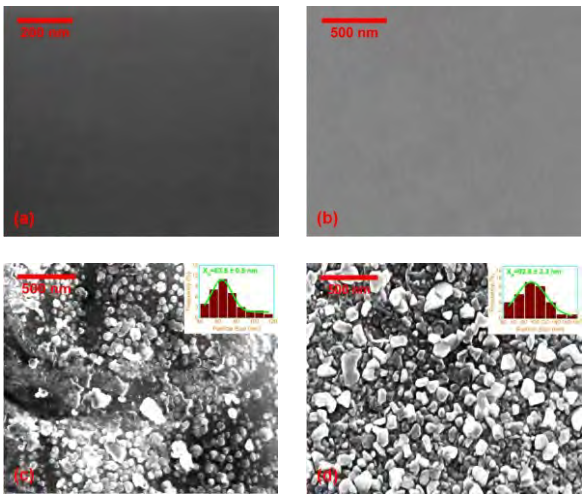

Fig. 9. Microstructures of $Fe_{71.5}Nb_5Cu_1Si_{13.5}B_9$ annealed at **(a)** 500ºC, **(b)** 550ºC, **(c)** 600ºC and **(d)** 650ºC temperatures.

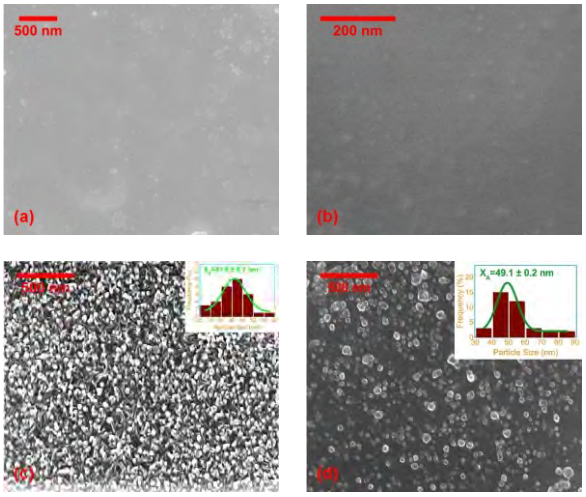

Fig. 10. Microstructures of $Fe_{69.5}Nb_7Cu_1Si_{13.5}B_9$ annealed at **(a)** 500ºC, **(b)** 550ºC, **(c)** 600ºC and **(d)** 650ºC temperatures.

Apart from this, the smallest grains in an average (41nm) are observed for the composition $Fe_{69.5-x}Nb_7Cu_1Si_{13.5}B_9$ annealed at 600°C which is found to be enlarged to 49.1 nm for T_a = 650°C. In general, Cu acts as a nucleation agent in the Finemet® alloys while Nb hinders grain growth. Therefore, the grain growth is favored by the combined effect Nb and α-Cu, as well as their low solubility in α-Fe(Si) [27]. Besides, the inclusion of Cu and Nb in Fe-Si-B based alloys causes ultrafine α-Fe(Si) nanoparticles to disperse in an amorphous matrix, averaging out the magneto-crystalline anisotropy energy [28, 29], and high permeability is acquired in these alloys. Moreover, a strong magnetic exchange coupling between the nanograins may result from the scattered and identical grains involved due to annealing. G. Herzer reported that the magnetic domain of the nanocrystal can easily be rotated if the size of the grains is ~12 nm [17]. Finally, a homogeneous microstructure with 41.0 nm grains is achieved for the sample x = 7 through a thermal treatment of T_a = 600°C and could be a suitable candidate for the magnetic application.

C. Hardness Testing

The hardness of metals or alloy material determines the strength of these, and it is a property that is resistive to localized plastic deformation. In general, the alloys are harder than any pure metal because they are prepared with the addition of different pure metals to enhance their properties. Fig. 11 represents the hardness testing apparatus and nanoindentation has been implemented on the ribbon-shaped sample of the highly crystalline samples.

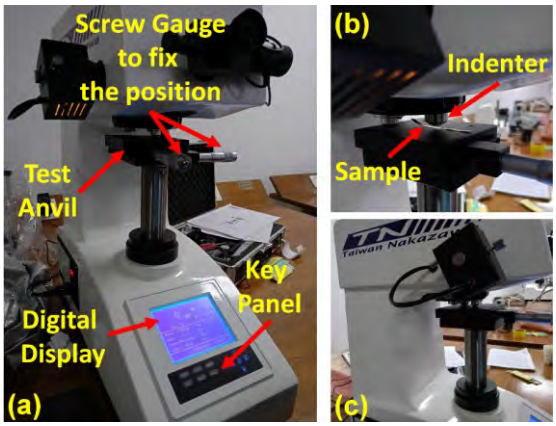

Fig. 11. Hardness testing process showing **(a)** the components of the apparatus, **(b)** testing of the Finemet ribbon by the indentation method, and **(c)** side view of the machine displaying the model's name.

The hardness of these samples has been measured at three different locations (defined as A, B, and C) for each sample. Fig.12 displays the values of hardness measured for the composition $Fe_{76.5-x}Nb_xCu_1Si_{13.5}B_9$ with x = 1, 3, 5, and 7 annealed at 650°C. The measured hardness values have been averaged and the highest value is obtained for the sample x = 1 (~40.7 GPa) for which the grains are the largest. The Hall-Petch relationship provides a good representation of the hardness of large-grained materials, showing that the hardness variation is proportional to the grain sizes [30]. Therefore, the studied samples might establish a linear relationship between these factors. Here, in the samples x=5 and x=7, the hardness of x=5 is higher (~28.3 GPa) than that of x=7 (~24.4 GPa), and the grain size of x=5 (~92.8 nm) is also larger than that of x=7 (~49.1 nm) when annealed at the 650°C (Table-II). However, according to the Hall–Petch relationship samples with lower grain sizes have higher tensile strength and ductility as well as lower hardness.

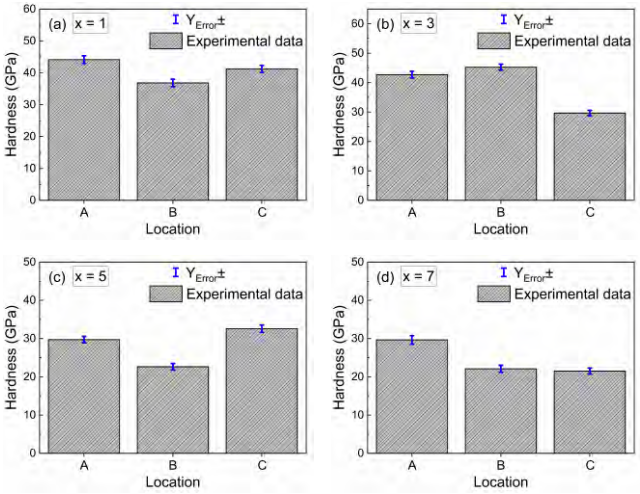

Fig. 12. Variation of hardness at different locations of the sample with the composition $Fe_{76.5-x}Nb_xCu_1Si_{13.5}B_9$ where, **(a)** x = 1, **(b)** x=3, **(c)** x=5 and **(d)** x=7 annealed at 650°C temperatures.

Apart from this, the hardness of the synthesized nanocomposite soft magnets has been studied concerning the volume fraction of the crystalline phase (VFC), rather than the grain size. Fig. 13 represents the variations of hardness with VFC for the composition of $Fe_{76.5-x}Nb_xCu_1Si_{13.5}B_9$ alloys with x = 1, 3, 5, and 7 annealed at 650°C temperatures.

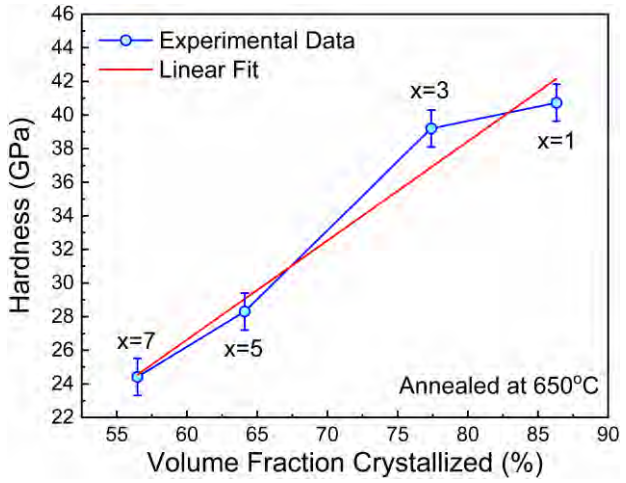

Fig. 13. Variation of Hardness as a function of crystalized phase fraction (%) for the composition $Fe_{76.5-x}Nb_xCu_1Si_{13.5}B_9$ alloys where, x = 1, 3, 5 and 7 annealed at 650°C temperatures.

A nearly linear relationship between hardness and VFC is shown in Fig. 13, indicating that VFC influences hardness. The sample x=1 has the highest value of VFC (86.3%) resulting in the maximum hardness. However, a material with more hardness tends to be more brittle and breaks or cracks more easily under stress rather than deforming. Conversely, a ductile material can absorb more energy by deforming before it breaks, but it usually has lower hardness. Therefore, the sample x=7 with lower hardness is more suitable for the practical application. Finally, annealing at a higher temperature reduces strain in the densely packed atoms of the amorphous matrix, likely due to higher Nb concentrations, and improves the sample's ductility as its hardness decreases.

IV. CONCLUSIONS

In this communication, we have successfully found out the interplay between Nb doping and the thermal treatment of a Finemet® alloy system. Heat treatment enhances the crystalline phase whereas Nb addition to the alloy tends to suppress the crystal growth. Therefore, control over the crystallographic structure could be achieved, which is important for tuning and/or enhancing the physical properties of any Finemet® alloy for the application. Finally, the composition $Fe_{69.5}Nb_7Cu_1Si_{13.5}B_9$ annealed at 650°C seems to be more suitable for its lowest hardness (~24.4 GPa) as well as enhanced ductility along with 86.3% crystalline phase.

V. REFERENCES

[1] Y. Yoshizawa, S. Oguma, K. Yamauchi, "New Fe-based soft magnetic alloys composed of ultrafine grain structure," *J. Appl. Phys.*, vol. 64, pp. 6044, 1988, https://doi.org/10.1063/1.342149

[2] Haibo Sun, Zhili Guo, Zukun Liang, Weihong Chen, Qingtao Zeng, Ce Wang, "Enhancements of preparation efficiency and magnetic properties for Fe-based amorphous magnetic flake powder cores upon the adoption of a novel double-paralleled slits nozzle," *J. Magn. Magn. Mater.*, vol. 500, pp. 166358, 2020, https://doi.org/10.1016/j.jmmm.2019.166358.

[3] Yiqun Zhang, Qiang Chi, Liang Chang, Yaqiang Dong, Pingping Cai, Yan Pan, Mengji Gong, Jianjun Huang, Jiawei Li, Aina He, Xinmin Wang, "Novel Fe-based amorphous compound powder cores with enhanced DC bias performance by adding FeCo alloy powder," *J. Magn. Magn. Mater.*, vol. 507, pp. 166840, 2020, https://doi.org/10.1016/j.jmmm.2020.166840.

[4] Rongdi Guo, Guoliang Yu, Mingmin Zhu, Yang Qiu, Guohua Wu, Haomiao Zhou, "Regulation of magnetic and electrical performances in core-shell-structured FeSiCr@$BaTiO_3$ soft magnetic composites," *J. Alloys Compd.*, vol. 895, no. 2, 162724, 2022, https://doi.org/10.1016/j.jallcom.2021.162724.

[5] Giselher Herzer, "Nanocrystalline soft magnetic materials," *J. Magn. Magn. Mater.*, vol. 157–158, pp. 133-136, 1996, https://doi.org/10.1016/0304-8853(95)01126-9.

[6] Y. Yoshizawa, K. Yamauchi, "Magnetic properties of Fe–Cu–M–Si–B (M = Cr, V, Mo, Nb, Ta, W) alloys," *Mater. Sci. Eng. MAT SCI ENG A-STRUCT*, vol. 133, pp. 176-179, 1991, DOI:10.1016/0921-5093(91)90043-M

[7] T. Gheiratmand, H.R. Madaah Hosseini, "Finemet nanocrystalline soft magnetic alloy: Investigation of glass forming ability, crystallization mechanism, production techniques, magnetic softness and the effect of replacing the main constituents by other elements," *J. Magn. Magn. Mater.*, vol. 408, pp. 177-192, 2016, https://doi.org/10.1016/j.jmmm.2016.02.057.

[8] S. P. Mondal, Kazi Hanium Maria, S.S. Sikder, Shamima Choudhury, D.K. Saha, M.A. Hakim, "Influence of Annealing Conditions on Nanocrystalline and Ultra-Soft Magnetic Properties of $Fe_{75.5}Cu_1Nb_1Si_{13.5}B_9$ Alloy," *J. Mater. Sci. Technol.*, vol. 28, no. 1, pp. 21-26, 2012, https://doi.org/10.1016/S1005-0302(12)60018-8.

[9] Enayet Hossain, Shamima Choudhury, M. A. Bhuiyan, K. H. Maria, M. H. Mesbah Ahmed, D. K. Saha, M. A. Hakim, "Magnetic Softening of Nanocrystalline $Fe_{74}Cu_{1.5}Nb_{2.5}Si_{12}B_{10}$ Alloy by the Process of Annealing," *Adv. Sci. Focus.*, vol. 2, no. 1, pp. 12-16, 2014, DOI: https://doi.org/10.1166/asfo.2014.1063

[10] S. Manjura Hoque, M.A. Hakim, F.A. Khan, N. Chau, "Ultra-soft magnetic properties of devitrified $Fe_{75.5}Cu_{0.6}Nb_{2.4}Si_{13}B_{8.5}$ alloy," *Mater. Chem. Phys.*, vol. 101, no. 1, pp. 112-117, 2007, https://doi.org/10.1016/j.matchemphys.2006.02.023.

[11] Y. Zhang, Y. Wang and A. Makino, "NANOMET® and FINEMET®: Investigation on the crystallization mechanism between different kinds of Fe-based soft magnetic nanocomposite alloys," *2017 IEEE International Magnetics Conference (INTERMAG), Dublin, Ireland, 2017*, pp. 1-1, doi: 10.1109/INTMAG.2017.8007885.

[12] A. Zhukov, M. Ipatov, M. Churyukanova, A. Talaat, J.M. Blanco, V. Zhukova, "Trends in optimization of giant magnetoimpedance effect in amorphous and nanocrystalline materials," *J. Alloys Compd.*, vol. 727, pp. 887-901, 2017, https://doi.org/10.1016/j.jallcom.2017.08.119.

[13] A Zhukov, A. F Cobeño, J Gonzalez, A Torcunov, E Pina, M.J Prieto, J.M Blanco, V Larin, S Baranov, "Ferromagnetic resonance, magnetic behaviour and structure of Fe-based glass-coated microwires," *J.*

Magn. Magn. Mater., vol. 203, no. 1-3, pp. 238-240, 1999, https://doi.org/10.1016/S0304-8853(99)00240-1.
[14] A. Zhukov, M. Churyukanova, S. Kaloshkin, V. Semenkova, S. Gudoshnikov, M. Ipatov, A. Talaat, J.M. Blanco, V. Zhukova, "Effect of annealing on magnetic properties and magnetostriction coefficient of Fe–Ni-based amorphous microwires," *J. Alloys Compd.*, vol. 651, pp. 718-723, 2015, https://doi.org/10.1016/j.jallcom.2015.08.151.
[15] M. Churyukanova, V. Zhukova, A. Talaat, J.J. del Val, S. Kaloshkin, E. Kostitcyna, E. Shuvaeva, V. Sudarchikova, A. Zhukov, "Studies of thermal and magnetic properties of Fe-based amorphous and nanocrystalline glass-coated microwires," *J. Alloys Compd.*, vol. 615, no. 1, pp. S256-S260, 2014, https://doi.org/10.1016/j.jallcom.2013.12.030.
[16] M. Churyukanova, S. Kaloshkin, E. Shuvaeva, A. Mitra, A.K. Panda, R.K. Roy, P. Murugaiyan, P. Corte-Leon, V. Zhukova, A. Zhukov, "The effect of heat treatment on magnetic and thermal properties of Finemet-type ribbons and microwires," *J. Magn. Magn. Mater.*, vol. 492, pp. 165598, 2019, https://doi.org/10.1016/j.jmmm.2019.165598.
[17] Giselher Herzer, "Modern soft magnets: Amorphous and nanocrystalline materials," *Acta Mater.*, vol. 61, no. 3, pp. 718-734, 2013, https://doi.org/10.1016/j.actamat.2012.10.040.
[18] Ahmed Talaat, David W. Greve, M.V. Suraj, Paul R. Ohodnicki, "Electromagnetic assisted thermal processing of amorphous and nanocrystalline soft magnetic alloys: Fundamentals and advances," *J. Alloys Compd.*, vol. 854, pp. 156480, 2021. https://doi.org/10.1016/j.jallcom.2020.156480.
[19] Yaocen Wang, Yan Zhang, Akira Takeuchi, Akihiro Makino, Yoshiyuki Kawazoe, "Investigation on the crystallization mechanism difference between FINEMET® and NANOMET® type Fe-based soft magnetic amorphous alloys," *J. Appl. Phys., Vol.* 120, pp. 145102, 2016, https://doi.org/10.1063/1.4964433
[20] Chao-Yang Tsao, Jürgen W. Weber, Patrick Campbell, Per I. Widenborg, D. Song, Martin A. Green, "Low-temperature growth of polycrystalline Ge thin film on glass by in situ deposition and ex situ solid-phase crystallization for photovoltaic applications," *Appl. Surf. Sci.*, vol. 255, no. 15, pp. 7028-7035, 2009, https://doi.org/10.1016/j.apsusc.2009.03.035.
[21] N. Ponpandian, A. Narayanasamya, K. Chattopadhyay, M. Manivel Rajab, K. Ganesan, C. N. Chinnasamy, B. Jeyadevan, "Low-temperature magnetic properties and the crystallization behavior of FINEMET alloy," *J. Appl. Phys.*, Vol. 93(10), pp. 6182-6187, 2003, https://doi.org/10.1063/1.1565829
[22] E. F. Keskenler, M. Tomakin, S. Doğan, G. Turgut, S. Aydın, S. Duman, B. Gürbulak, "Growth and characterization of Ag/n-ZnO/p-Si/Al heterojunction diode by sol-gel spin technique," *J. Alloys Compd.*, vol. 550, pp. 129-132, 2013, https://doi.org/10.1016/j.jallcom.2012.09.131.
[23] O. Volnianska, P. Boguslawski, J. Kaczkowski, P. Jakubas, A. Jezierski, E. Kaminska, "Theory of doping properties of Ag acceptors in ZnO," *Phys. Rev. B*, vol. 80, no.24, pp. 245212, 2009, DOI:10.1103/PhysRevB.80.245212
[24] Zhi Wang, Jing Yang, Ye-mei Han, Dong-xu Zhang, Bin Fu, Rongchang Ye, "Magnetostriction and effective magnetic anisotropy of Co-contained Finemet nanocrystalline alloys," *J. Appl. Phys.*, vol.107, pp. 09A308, 2010, https://doi.org/10.1063/1.3340514
[25] X. Y. Zhang, F. X. Zhang, J. W. Zhang, W. Yu, M. Zhang, J. H. Zhao, R. P. Liu, Y. F. Xu, W. K. Wang, "Influence of pressures on the crystallization process of an amorphous $Fe_{73.5}Cu_1Nb_3Si_{13.5}B_9$ alloy," *J. Appl. Phys.*, vol. 84, pp. 1918, 1998, https://doi.org/10.1063/1.368319
[26] Md Khalid Hossain, Jannatul Ferdous, Md Manjurul Haque, A. K. M. Abdul Hakim, "Development of Nanostructure Formation of $Fe_{73.5}Cu_1Nb_3Si_{13.5}B_9$ Alloy from Amorphous State on Heat Treatment," *World J. Eng.*, vol. 5, no. 4, pp. 107, 2015, DOI:10.4236/wjnse.2015.54013
[27] Yurong Jia, Zhi Wang, Fang Wang, Li Zhang, Hongjun Duan, "Effect of Ti on structure and soft magnetic properties of Si-rich Finemet-type nanocrystalline $Fe_{73.5}Cu_1Nb_{3-x}Si_{17.5}B_5Ti_x$ alloys," *Mater. Res. Bull.*, vol. 106, pp. 296-300, https://doi.org/10.1016/j.materresbull.2018.06.018.
[28] Seul-Ki Nam, Sun-Gyu Moon, Keun Yong Sohn, Won-Wook Park, "Microstructural Change and Magnetic Properties of Nanocrystalline Fe-Si-B-Nb-Cu Based Alloys Containing Minor Elements," *J. MAGN.*, vol. 19, no. 4, pp. 327-332, 2014, https://doi.org/10.4283/JMAG.2014.19.4.327
[29] N. Chau, N. Q. Hoa, N. D. The, L. V. Vu, "The effect of Zn, Ag and Au substitution for Cu in Finemet on the crystallization and magnetic properties," *J. Magn. Magn. Mat.*, vol. 303, no. 2, pp. e415-e418, 2006, https://doi.org/10.1016/j.jmmm.2006.01.057.
[30] S. N. Naik, S. M. Walley, "The Hall–Petch and inverse Hall–Petch relations and the hardness of nanocrystalline metals," *J. Mater. Sci.*, Vol. 303, pp. 2661-2681, 2020, https://doi.org/10.1007/s10853-019-04160-w

First Dr. Md. Masud was born in Natore District, Bangladesh, in 1972. He obtained his B.Sc. and M.S. degrees in Physics from Jagannath University, Dhaka, Bangladesh in 1994 and 1995, respectively. In 2008, he completed his M.Phil. in Condensed Matter Physics from the University of Dhaka. He earned his Ph.D. in Theoretical Physics from the University of Dhaka in 2021, supported by a fellowship from the International Science Programme (ISP) of Uppsala University, Sweden. Dr. Rana has experimentally validated several theoretical models in materials science, including studies on Finemet ribbons and nanomaterials. Since 2011, he has been serving as an Associate Professor in the Department of Computer Science and Engineering at Mohammadpur Kendriya College, Dhaka. He led several research projects funded by the Ministry of Science and Technology, Bangladesh, including work on energy-gap measurement tools, a digital trainer board, and an acoustic transducer. Dr. Rana was visiting research fellows of the Abdus Salam International Centre for Theoretical Physics (ICTP), Italy, in 2003, and at the Vietnam Academy of Science and Technology (VAST) in 2011. His research interests are theoretical condensed matter physics, health and radiation physics in both experimental and theoretical domains.

Second Dr. Md. Sarowar Hossain was born at Kachiapar village, Sandip Upazila, Chattogram District, Bangladesh in 1983. He received B.Sc. and M.S. degrees in Physics form Shahjalal University of Science and Technology, Sylhet Bangladesh, in 2008 and 2009, respectively. He worked as a project fellow at the Bangladesh Atomic Energy Centre, Dhaka, from March to August 2009, completing his M.S. thesis on dielectric materials. He received Ph.D. from University of Calcutta under the fellowship of TWAS-Bose Postgraduate award, ICTP, Italy and awarded on 23rd March 2021. He was a senior research fellow from S N Bose National Centre for Basic Sciences, Kolkata, India affiliated with Department of Science and Technology (DST), India from April 2014 to October 2019. Since 2023, he has been working as an Assistant Professor in the Department of Physics, American International University-Bangladesh, Dhaka, Bangladesh. His research interests are dynamic elastic properties, thermo-magnetization, magnetic susceptibility and hysteresis, photo/stress induced micro-actuation and transport properties exhibited by ferromagnetic shape memory alloys and disordered magnetic alloys; magneto-dielectric properties of spinel ferrites, perovskite materials and hexaferrites. His research work includes 39 peer-reviewed journal articles with over 600 citations and has been presented at more than 35 national and international conferences. He is a reviewer of *Journal of Alloys and Compounds and The European physical journal*.

Third Dr. Md. Ehasanul Haque was born in Rajshahi, Bangladesh in 1986. He received B. Sc. and M. Sc. degrees in Materials Science and Engineering from the University of Rajshahi, Rajshahi, Bangladesh in 2008 and 2009 respectively. Dr. Haque earned his Ph.D. degree in Materials Science from Japan

Advanced Institute of Science and Technology (JAIST), Ishikawa, Japan in 2018. He started his teaching career as an Assistant Professor in American International University-Bangladesh, Dhaka, Bangladesh in May 2018. Currently, Dr. Haque is working as a Senior Assistant Professor and Head at the Department of Industrial and Production Engineering in American International University-Bangladesh. His research is focused on composite materials, electrodeposition techniques, nonlinear optics, alloy formation and microstructure study an.

Md. Rabiul Hassan was born in Barishal, Bangladesh, in 1991. He received his B.Sc. degree in Physics from Khulna University and his M.Sc. degree from Khulna University of Engineering & Technology (KUET). He has previously served as a faculty member in the Department of Physics at Northern University of Business & Technology, Khulna, and as a part-time faculty member in the Department of Physics, KUET, Bangladesh. He is currently working as a Scientific Officer at the Rooppur Nuclear Power Plant, Bangladesh. He has received advanced training in nuclear power plant operation and maintenance from Rosatom Technical Academy, Russia. He also participated in several international conferences and seminars held in Japan, India, and Nepal. His research expertise includes ceramic materials, nanomaterials, materials synthesis, and characterization.

Dr. Mehedi H. Rizvi received his B.Sc. and M.Sc. degrees in 2013 from Bangladesh University of Engineering and Technology (BUET). He began his academic career the same year as a Lecturer at BUET and was promoted to Assistant Professor in 2015. In 2018, he began his Ph.D. in Materials Science at North Carolina State University, which he completed in 2022. Throughout his academic journey, he received several prestigious honors, including the Prime Minister's Gold Medal for outstanding undergraduate achievement and the Graduate Merit Award for excellence during his Ph.D. studies. He is currently working as a Senior Research Engineer at Corning Incorporated, New York, USA.

Dr. Mohammed Nazrul Islam Khan was born at Shariatpur District, Bangladesh. He received B.Sc. and M.S. degrees in Physics form Jagannath University, Dhaka, Bangladesh. He completed the M.Phil. degree from Bangladesh University of Engineering and Technology (BUET) and later obtained Ph.D. in Applied Physics from Tohoku University, Japan, specializing in magnetic and nanostructured materials. He began his professional career at the Atomic Energy Centre, Dhaka (AECD), where he currently serves as a Chief Scientific Officer in the Materials Science Division. His core research areas include nanotechnology, magnetism, dielectric materials, analytical spectroscopy, and X-ray diffraction. He was a leading contributor to the Ambient Air Quality Monitoring Project in Dhaka, which provided critical scientific evidence leading to the removal of leaded petrol from Bangladesh in 1999. He has also led impactful research in trace element analysis using sophisticated techniques such as PIXE, XRF, TXRF, and AAS. His research work comprises more than 200 peer-reviewed journal publications with over 4,000 citations and has been presented at numerous national and international conferences. He also serves as a reviewer and editorial board member of several reputed journals. Dr. Khan's contributions to science have been recognized with multiple prestigious awards, including the Khwarizmi International Award (1993) and the Bangladesh Academy of Sciences Gold Medal (1993) in Physical Sciences (Senior Group). He is currently serving as the General Secretary of the Bangladesh Physical Society, contributing significantly to the academic and scientific community of the country.

Dr. Abu Zafur Ziauddin Ahmed was born at Dhaka, Bangladesh in 1972. He received B.Sc. and M.S. degrees in Physics form Jagannath University, Dhaka, Bangladesh in 1994 and 1995, respectively. He is a distinguished academician and renowned researcher specializing in theoretical condensed matter physics. He has developed deep expertise in quantum simulation and, in recent years, has expanded his research focus to include nuclear materials science. In addition to his theoretical work, he actively collaborates with experimental research groups, contributing to interdisciplinary studies. His proficiency in parallel computing and data science further enhances his research capabilities and impact.

Dr. M. A. Hakim was born in Naogaon District, Bangladesh. He received B.Sc. and M.Sc. degrees in Metallurgical Technologies from Belarusian National Technical University, Minsk, Belarus between 1973 to1978. He received the Ph.D. in Magnetic Materials from BUET and split-site research at Uppsala University, Sweden in 1995. He was a former director of the Bangladesh Atomic Energy Commission and former visiting professor at the Department of Nanomaterials and Ceramic Engineering at the Bangladesh University of Engineering and Technology. He spent nearly 40 years in research and teaching roles at both BAEC and BUET, helping build capacity in nanomaterials science. His expertise spanned nanomaterials, magnetic materials, condensed matter physics, and advanced ceramics. As a senior scientist at the Bangladesh Atomic Energy Commission and a visiting professor at BUET, he published over 200 research papers and played a key role in advancing nanoscience in the country. Throughout his long career, he worked as visiting fellow at different organizations including -Indian Institute of Science (IISc) and Jawaharlal Nehru Centre for Advanced Scientific Research (JNCASR) in Bangalore, India; Vietnam Academy of Science in Hanoi, Vietnam; and International Science Programme (ISP) of Uppsala University in Sweden, Munster Technological University. He was former vice-president of Bangladesh Physical Society.